Seismic hazard associated to mine planning strategies: A novel application of the Gutenberg Richter distribution and the extreme value theory illustrated in a deep mine case study

by J. Jarufe[1], L. Alfaro[1], E. Rubio[2], C. Morante[3], C. Gómez[4], R. Cuba[4]

Affiliation:
1 Universidad de Santiago de Chile, Chile
2 Redco Santiago, Chile
3 Redco Lima, Peru
4 Compañia Minera Raura, Peru

Correspondence to:
J. Jarufe

Email:
juan.jarufe@usach.cl

Dates:
Received: 03 Jan. 2025
Revised: 23 Mar. 2026
Accepted: 05 Jul. 2026
Published: Aug. 2026

How to cite:
Jarufe J., Alfaro, L., Gómez C., Cuba R. Rubio E., Morante C. 2026. Seismic hazard associated to mine planning strategies, A novel Applications of the Gutenberg Richter Distribution and the Extreme Value Theory Illustrated in a Deep Mine Case Study. *Journal of the Southern African Institute of Mining and Metallurgy*, vol. 126, no. 8, pp. 455 – 466

DOI ID:
https://doi.org/10.17159/2411-9717/3638/2026

ORCiD:
J. Jarufe
https://orcid.org/0000-0003-2373-785X
C. Gómez
https://orcid.org/0009-0005-6061-4965

Abstract

The increasing global demand for metals compels the mining industry to optimise production methods and planning to meet rising needs. However, as mining operations extend deeper, the risks associated with mining-induced seismicity and rockburst hazards become more critical. Effectively managing mining rates is essential for controlling induced seismicity and mitigating these risks.

This paper presents a novel and practical methodology for integrating seismic hazard considerations into mine production planning. By analysing historical seismic and mine production data, the methodology develops actionable guidelines for addressing short-term planning challenges. In contrast to traditional reliance on unwritten miner experience or time-intensive numerical modelling solutions, this approach offers a streamlined and timely framework for decision-making.

The proposed framework is applied to a case study of a Peruvian polymetallic mine utilising the sublevel stoping method with backfill. The results demonstrate the methodology's ability to optimise short-term operational decisions, striking a balance between production efficiency and safety standards, and highlighting its potential for broader application in the mining industry.

Keywords

Seismicity, mine planning, seismic hazard, rockburst

Introduction

The relationship between the volume of extracted rock and induced seismicity is a fundamental aspect of assessing the geomechanical effects of mining operations. As mining activities intensify and progress to greater depths, the frequency and magnitude of seismic events tend to increase, underscoring the need for a comprehensive understanding of the underlying mechanisms.

The extraction of rock alters the stress distribution within the surrounding geological structures. This redistribution of stress can trigger the reactivation of pre-existing faults (Potvin et al., 2010) or induce the formation of new fractures. These changes may result in seismic events that range from minor tremors to significant fault displacements, particularly in proximity to critical underground infrastructure.

A thorough understanding of the interplay between mined volume and seismicity is crucial for developing robust mitigation strategies. Such strategies aim to ensure operational safety, minimise the risk of damage to infrastructure, and maintain the long-term stability of mining operations.

Stress changes resulting from mining activities are inherently complex and influenced by multiple factors, including the depth of extraction, the chosen mining method, geological conditions, and the mining rate. Deeper mining operations are associated with more pronounced seismicity due to the elevated stress conditions characteristic of greater depths.

Mining methods that involve large-scale rock removal, such as block caving, typically cause significant stress redistributions when compared to more controlled methods like open stoping or room-and-pillar mining (Wagner, 2019; Wang et al., 2009). Furthermore, the mechanical properties of the surrounding rock mass are critical; brittle rocks, in particular, are more susceptible to sudden failure, potentially triggering seismic events (An, Mu, 2024).

Effective management of induced seismicity in mining environments involves a combination of real-time monitoring, predictive modelling, and engineering controls. Seismic monitoring networks are essential for detecting and analysing seismic events, providing valuable data that can be used to adjust mining operations and mitigate risks (Mendecki 2023). Additionally, understanding the relationship between mined volume and induced seismicity allows for the development of predictive models that can forecast seismic events based on mining activities and stress changes (Martinsson et al., 2020; Das Jennifer et al., 2022; Khalil et al., 2022). By integrating these approaches, mining companies can better manage the risks associated with induced seismicity, ensuring safer and more sustainable operations.

Mine planning and seismic hazard

The mine planning design process is a critical engineering stage that defines the appropriate mining units, such as stope size, block caving undercut area, and pillar size, as well as the rate at which the mine will be extracted. These two factors are closely related, as the size of the mining units and supporting infrastructure will determine the rate at which material can be drawn from the mine. Additionally, the mine must produce a predefined amount of ore to meet the capacity of the processing plant, ensuring the mine and plant operate at full production without bottlenecks in the overall process.

The mine plan design process begins with an initial approach generated by the planning department, which is guided by factors such as mineral grade distributions, the economic value of the mine sequence, and empirical geotechnical design guidelines. These guidelines include methods for determining stope dimensions, pillar design, and the minimum required cave area. While these empirical techniques help control the geometry of the excavations and pillars to achieve the desired production rate, they do not consider the potential for seismic activity and rockburst hazards. To address these risks, rock mechanics engineers analyse the planning sequence using numerical modelling and provide feedback to the mine planning team, leading to modifications of the initial design to mitigate the identified hazards that could not be evaluated using the standard empirical tools.

While the resulting mine sequence has the geotechnical and economical backup to satisfy project needs, it is common that during the operational stage of the mine, where the final results from the planning-geotechnical design are being implemented into the mine, some changes to the accepted planning scheme had to be made. These are usually related to unforeseen conditions such as variations in ore grades, geotechnical conditions or operational factors such as low availability of mining equipment among other reasons. All of these situations generate changes in the mine sequence that cannot always go through a detailed rock mechanics review due to the extensive response times that geotechnical analysis requires.

Based on the previous discussion, it would be more useful to the planning department to have design tools to allow the generation of planning decisions based on the expected seismic response of the rockmass.

Rockburst and seismic activity are inherent consequences of extensive mining deep underground (Cook, 1976). The relationship between mining activities and seismicity has been well-established through numerous historical examples from mining regions around the world. In the Upper Silesia mines in Poland and the Brezove Hoty district in Czechoslovakia, the rockburst phenomenon has been extensively studied and documented, with researchers elaborating on the relationships between extracted rock volume and seismicity (Gibowicz, 1963; Gibowicz, Kijko, 1994; McGarr, 1976; Głowacka, Kijko, 1989; Glowacka, 1993; Vatcher et al., 2019). These studies have demonstrated the inherent connection between the intensity of mining operations and the resulting seismic events (Figure 1), highlighting the need for careful planning and management to mitigate such risks.

In South Africa, the mining industry has a long history of dealing with seismic hazards, which have been extensively researched and documented (Cook, 1976; McGarr, 1976; Ortlepp, 1997; Gibowicz, Kijko, 1994), where the inherent relationship between mining and seismicity was recognised not only on the energy released but also in the temporal distribution of seismicity after blasting (Cook, 1976).

The relationship between mining activities and seismic hazards has been well-documented in Canadian mines as well. Hasegawa et al. 1989 and Blake and Hedley (2003) reviewed several case studies of rockbursts in Canadian mines, concluding that high extraction ratios were often associated with large seismic events and rockbursts.

For example, in the Sudbury mining district of Ontario, Canada, a long history of seismic events and rockbursts has been observed. The Creighton Mine, one of the deepest mines in the region, has experienced numerous seismic events over the years, some of which have resulted in significant damage and fatalities. Researchers have attributed these seismic events to the high extraction ratios and the deep, high-stress mining environment. Similarly, in the Timmins mining camp of northern Ontario, the Hollinger and McIntyre mines have also grappled with seismic hazards. These mines, which operated at depths exceeding 2,000 metres, experienced numerous rockbursts that were linked to the high stresses induced by the extensive underground excavations. An example of this relationship can be seen in Figure 2, where increases in the occurrence of rockbursts (continuous black line) is related to increments of the mined tonnes (dashed line).

Quantitative relationships between mined rock and seismic hazard were established by Glowacka and Kijko (1989), where the seismic energy (commonly used in Polish mines) was found to be directly proportional to the volume of rock extracted, following Equation 1.

$$\sum E = C * \Delta V^B \quad [1]$$

Where $\sum E$ corresponds to the expected seismic energy, ΔV is the extracted rock volume, C and B are constants dependent of rockmass conditions.

The results from Equation 1 represent the most likely energy release value for a given volume of extracted rock. However, the authors suggest considering a normal distribution around the

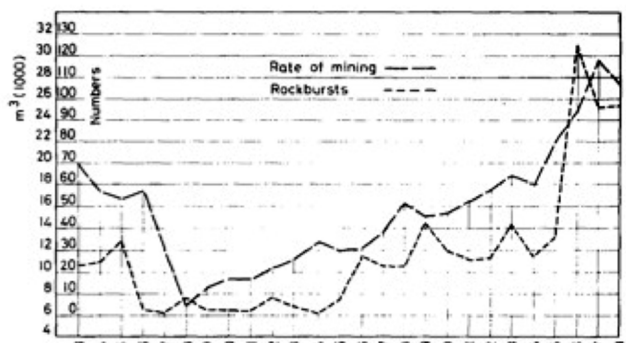

Figure 1—Relationship between rockburst incidence and mined volume for the Brezove Hoty mine district in Czechoslovakia (Cook, 1976)

calculated seismic energy (ΣE) value to account for the inherent variability in mining-induced seismic events. Following this concept, the probability P(Ej) of a seismic event with energy greater than a specific threshold P(ΣE > Ej) can be calculated using the cumulative normal distribution function, as shown in Equation 2. This quantitative relationship between mined rock volume and seismic hazard offers mine planners a valuable tool to incorporate seismic risk assessment into the mine planning process.

$$P(E_j) = 1 - \left(\frac{1}{\sigma\sqrt{2\pi}}\right) \int_0^{E_j} e^{-\frac{1}{\sigma^2}(E-\Sigma E)^2} dE \quad [2]$$

A more in-depth analysis on the relationship between mining and seismicity is provided by Mendecki and Lötter (2011) and Mendecki (2013), where it is proposed to express seismic hazard in terms of the extracted rock volume or, as the "inter-event expected volume" defined as the average volume mined to produce a seismic event above certain size. This method in conjunction with the Gutenberg and Richter (1956) relationship allows the calculation of the probability of experiencing a seismic event with a seismic potency (Mendecki 2016) greater than a specific value for a given inter-event extracted rockmass volume (Figure 3).

The results from the method proposed by Mendecki and Lotter (2011) and Mendecki (2013) describe the probability of experiencing a seismic event based on the available data and the corresponding Gutenberg and Richter (GR) model. Since the same GR model can be present infinite realisations, the distribution of the maximum values of each realisation can be modelled through the extreme value theory, where the probability that a magnitude x will be the largest among n independent samples from a random variable X with distribution F(x) is given by Gibowicz and Kijko (1994), Mendecki (2016), and Wesseloo (2020):

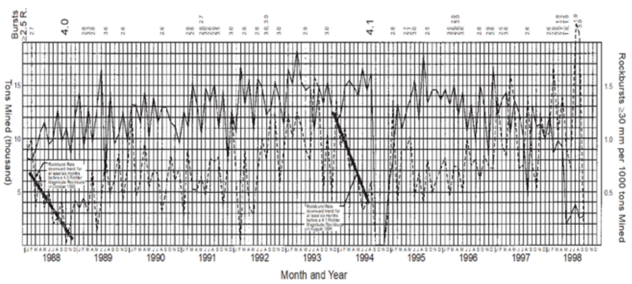

Figure 2—Seismicity and blasted volume (tonnes) in Lucky Friday Mine (Blake, Hedley. 2003)

$$F_{max}(x) = P(X_1 \leq x, X_2 \leq x, \ldots, X_n \leq x) = [F(x)]^n, \quad [3]$$

The results from Equation 3 provide a probabilistic outcome from the GR model, as shown by Mendecki (2016) in Figure 4.

Creating empirical mine design guidelines

The previous section described methods to calculate seismic hazard based on the GR parameters. Also, it was established that in many mine operations a relationship between mined volume and seismicity can be determined, as shown in Figure 1 and Figure 2. Finally, as discussed previously, a method to evaluate the seismic hazard based on mine planning alternatives would improve short-term decision in mine planning and also be an improvement in the design process since the beginning of the design.

In the present work, a method to evaluate and compare the seismic hazard of different mine planning scenarios is proposed and discussed. The mine planning scenarios correspond to different monthly mining rates and the seismic hazard is calculated based on past induced seismic history.

To evaluate seismic hazard associated with a planning option there are several steps that need to be completed, corresponding to the relationship between mining and seismicity, the amount of total seismicity generated by each mine plan scenario and the evaluation of the seismic hazard for each plan. These steps are detailed in the following section, and illustrated through a case study later in this paper.

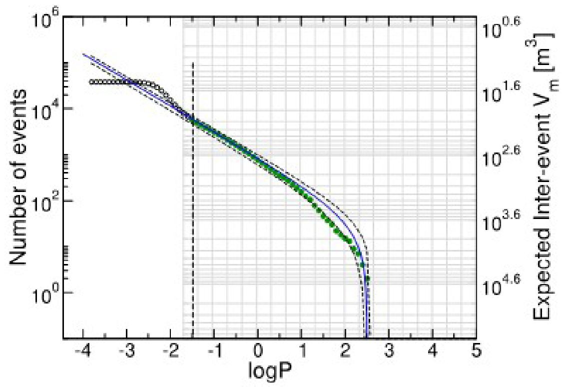

Figure 3—Frequency magnitude relationship with Gutenberg and Richter model and seismic potency (Log P) linked to the inter-event extracted volume on the right vertical axis (Mendecki, Lotter, 2011)

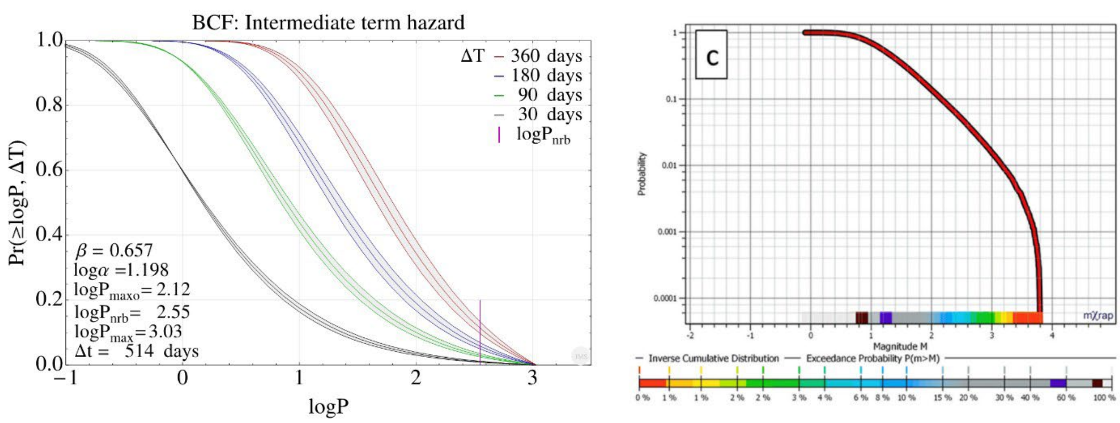

Figure 4—Seismic hazard estimation based on the GR parameters and the extreme value theory. Left: probability of exceeding a specific Log P value (Mendecki, 2016) Right: probability of exceeding a specific moment magnitude (Jarufe et al., 2022)

Identify failure mechanism associated with the future mine scenarios

As described by Hudyma and Potvin (2010) and in Hudyma (2010) (Figure 5), different mine environments react differently to the mine excavations, but also, variations in the mine sequences generate a different seismic response even for the same rockmass (Orlecka-Sikora et al., 2012; Malovichko, 2020). Of course, this occurs because of the different stress distribution caused by the different mine sequences. For the methodology considered in this paper, it is necessary to identify different failure mechanism domains, which may be defined by rockmass conditions or by the applied mining method.

Relationship between mined volume and seismicity

In this step, a relationship between mined rock volume and induced seismicity is established. Since seismic moment, representing the deformation at the seismic source, has been considered as one of the most reliable parameters (Glazer, 2016), it will be considered in this paper, however seismic potency (Mendecki, 2013) or apparent volume (Van Aswegen, Butler, 1993) can also be utilised. The relationship between mined volumes and seismicity can be calculated from the mine's existing data or utilising benchmarked values as the ones described by Vallejos and McKinnon (2011) or Mendecki (2012) among others (Figure 5).

It is important that, as described in the previous sections, relationships between mined volume and seismicity are based on the same rupture mechanism, considering a zonification of the seismic response domains to perform this analysis.

Calculate total seismicity for different mine planning scenarios

Applying the relationship between seismic response and mined volume, the total seismicity generated by different planning scenarios can be calculated. The planning scenarios are usually expressed as different daily production schemes in different mine sectors, however, to calculate the seismic hazard it is necessary to calculate the seismic moment associated to each planning scenario. This step is illustrated in Figure 7, where the mining rate for different stope scenarios, as described by Viljoen et al. (2021) has to be transformed into a monthly seismic moment for each planning scenario.

Develop probabilistic hazard model associated to each planned scenario

The total seismic moment is a representation of the total seismic deformation related to a specific mining scenario. This deformation does not occur as a single rupture but as a family of ruptures with an exponentially distributed failure radius, which is equivalent to a set of synthetic seismic events that, in total, generate the same fracturing as the total seismic moment calculated in the aforementioned step . The procedure to develop the synthetic distribution of events is described in Jarufe et al. (2022) but basically consists of generating a set of exponentially distributed seismic magnitudes of which the sum is equivalent to the total calculated seismic moment. This is done through an error minimisation procedure easily carried out with Excel Solver. Once the synthetic seismic data is generated, a and b values can be calculated and the Mmax distribution can be calculated as described through Equation 3 (Gibowicz, Kijko, 1994; Wesseloo, 2020).

The result from this methodology is the probability that the maximum magnitude will exceed a specific value, for each mine planning option.

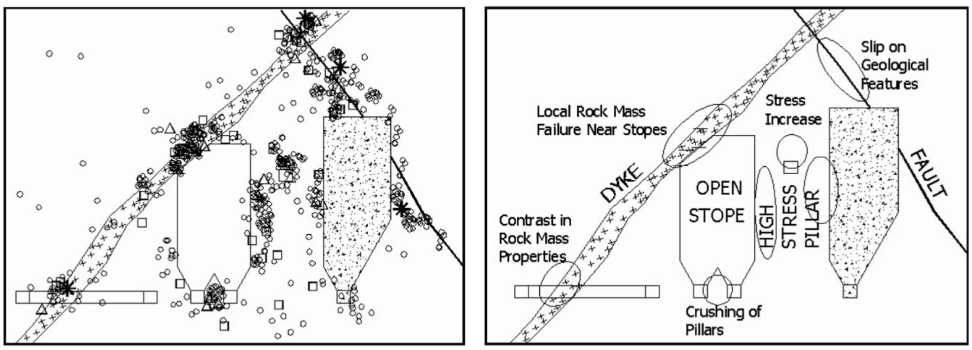

Figure 5—Different source mechanism around stope mines (Hudyma, 2010)

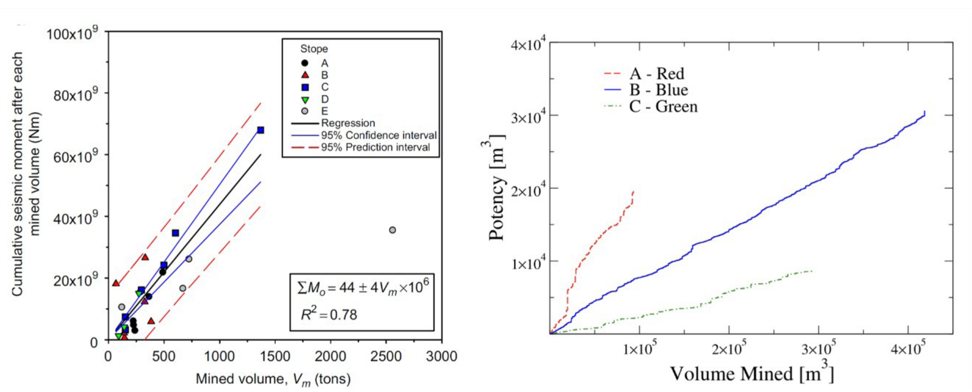

Figure. 6—Relationship between mined volume and seismic moment for Canadian mines (Vallejos, McKinnon, 2011) and mined volume with potency for South African mines (Mendecki, 2013)

The previous methodology will be illustrated through a case study of Raura mine in Peru, which during its deepening process faced relevant seismic events of increasing frequency as well as instabilities detected near blast sites. Faced with this situation, an analysis was done on the seismic rupture mechanisms, which can affect the deposit and the relationship between short-term production and rockmass seismic response.

Case study, open stope Raura mine 2023 backanalysis

Background information

Location and geological context

Raura mine is located in the Oyón district, 181 km northeast from the city of Lima, capital city of Peru. Geographically, the Raura mine lies on the peaks of the Raura Range, forming part of the watershed between the Pacific basin rivers and the Atlantic basin rivers, at a height ranging from 4300 to 5700 metres above sea level.

The Raura mining deposit has had a long industrial trajectory from colonial times with mine prospecting work along silver veins. Beginning in 1928, the mine underwent intense exploration until 1961, at which time the Compañía Minera Raura S.A. began its operations. The current plant capacity is 2,880 t/day.

The geological context of the Raura deposit is preceded by various geological events that took place within a complex structural framework, involving multiple tectonic repetitions. The Raura deposit is a skarn with polymetallic characteristics (Cu-Zn-Pb-Ag), and the mineral occurrences are associated with porphyritic stock of possible Miocene age and Cretaceous sedimentary units associated with the principal fault directions (Figure 8).

Mineralisation in veins is probably associated with a NE-SW longitudinal faults' direction, which have led to shear zones. The mineralisation has only moved to fill in faults with a NEE direction, because at the moment of mineralisation, the direction of maximum stress was NEE and the transversal fault jumps have not been played as extensional, but as transcurrent. In any case, mineralisation has circulated along the transversal faults, but the open spaces were small, and deposits have only been isolated or non-continuous. Silver, zinc, and copper appeared in lesser quantities, with more lead and zinc content in minerals towards the south (Figure 9).

The mine can be subdivided into three sectors: the Catuva zone located in the central part, which has several sectors that have already been mined; the Esperanza zone in the north, which includes several small-volume satellite structures; and the Hadas zone, which is the sector with the greatest reserve volume, the deepest sector, and where mining currently takes place.

Rockmass characteristics

The rock mass quality in various mineralised and sterile zones is assessed using diamond core samples, which include records of quality parameters for the rock mass. These records support geomechanical classifications such as the Bieniawski RMR and Barton's Q system. Additionally, geotechnical mapping across different zones evaluates rock mass quality and minor structural features (REDCO, 2021).

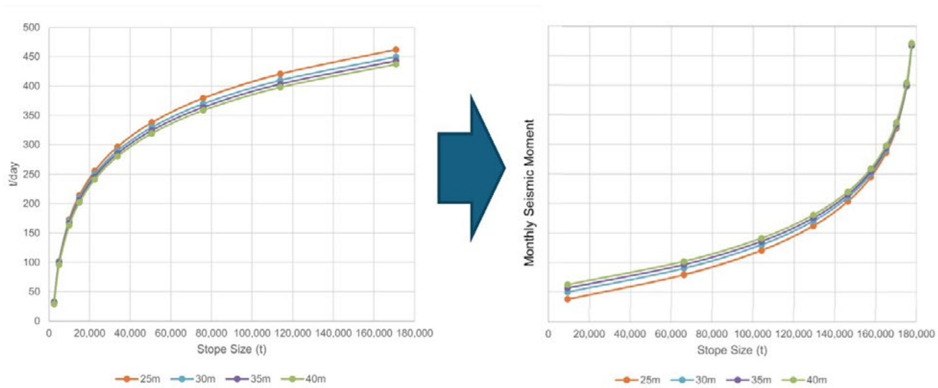

Figure. 7—Example of daily mined tonnes for different stoping options (as described by Viljoen et al., 2021) converted to an estimation of the seismic moment estimation for each planning scenario

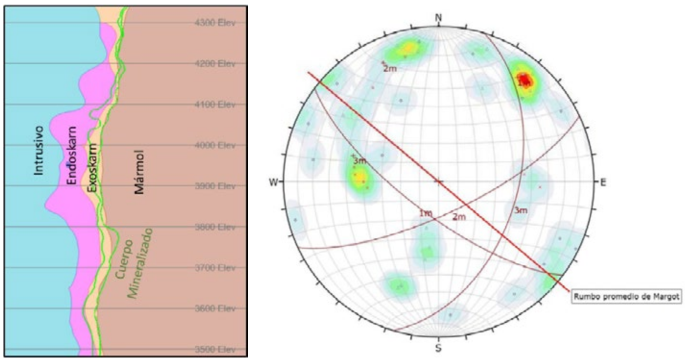

Figure. 8—Structural map of the Raura mining unit

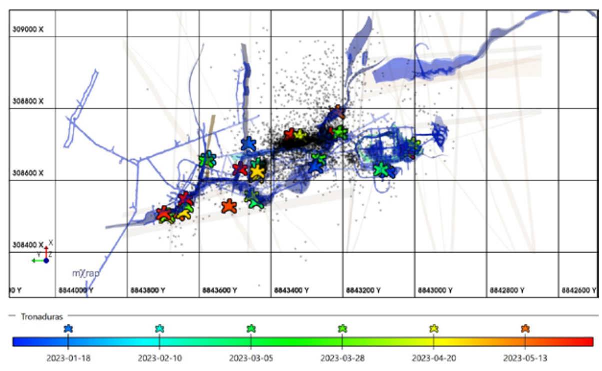

Figure 9—Plan view of the mineralised structures in the Raura mining unit. Dots indicate seismic events and stars corresponds to blast locations

To characterise the sectors of the Raura mine, the area can be subdivided into four distinct sectors according to Barton's classification (Figure 10). The Sur Alta zone comprises rock of fair to poor quality; the Norte Alta zone contains rock of fair to good quality; the Sur Baja zone features rock of fair to poor quality; and the Norte Baja zone includes rock of fair quality. It is noteworthy that the transition between the Alta and Baja zones occurs approximately at the 4100 elevation, while the boundary between the Sur and Norte zones varies gradually and is not defined by any specific structure. Seismicity is primarily observed within the mineralised bodies, likely due to mining operations activating pre-existing lithological and structural contacts within the mine.

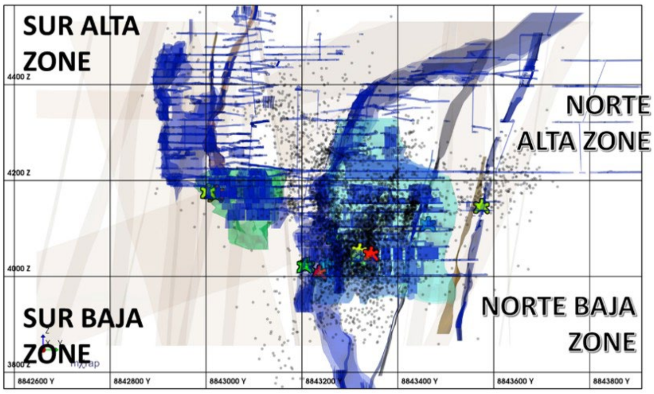

Figure 10—Raura geotechnical domains

Approximately 50 uniaxial rock tests were conducted to assess the strength characteristics of the rock samples, including intrusive, volcanic, porphyric, and limestones. The results of these tests showed a range of uniaxial compressive strength values, varying between 85 MPa and 120 MPa. This range indicates a moderate to high strength for the rock samples.

Mining method

Raura mine uses different mining methods depending on the geotechnical conditions. When the mineralised veins have low thickness (< 6m) and dipping up to 50°, bench and fill method is used (Figure 11a) for thicker sub vertical veins, pastefill stopes are considered, whereafter primary stopes are mined they are paste filled and secondary stope extraction occurs (Figure 11b).

Stress conditions derived from numerical modelling

Numerical finite element stress models have been developed and calibrated through back analysis in specific sectors of the mine where stress damage on excavations has been observed. This process enables the visualisation of stress anisotropy, as illustrated in Figure 12. Calibration results indicate that the induced principal stresses σ1 and σ3 are oriented with an azimuth of 130°, perpendicular to the tunnel direction in the evaluated section (Figure 12). The principal stress σ1 exhibits a plunge of 65°, resulting in minor to moderate damage to the structural bending located on the eastern side of the excavation. This enhanced understanding of stress distribution is crucial for improving the design and safety of mining operations.

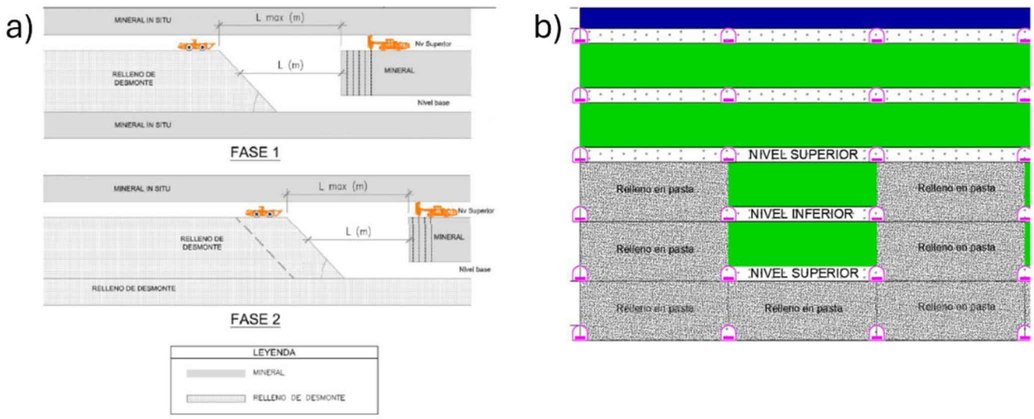

Figure 11—Mining methods used in Raura mine. a) Bench and fill method, b) paste-filled stopes for sub- vertical veins (REDCO, 2021).

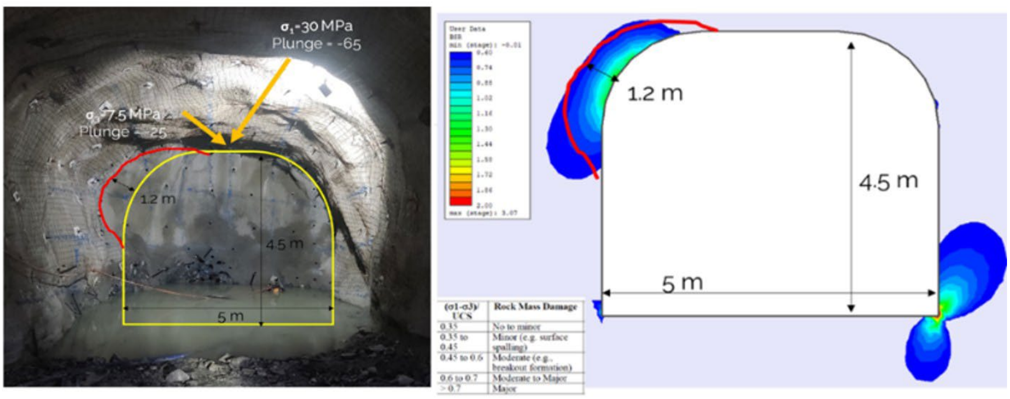

Figure 12—Principal stress calibration using 3D mine scale numerical modelling

This calibration of principal stresses was integrated into a comprehensive 3D global model of the mine, simulating the already mined and backfilled zones to determine the current induced stress conditions. The model also simulates the life of mine (LOM) mining sequence to predict future induced stress conditions according to the mining plan.

The magnitude of the maximum principal stress at the current mining levels, which are located between elevations 4000 and 4100, ranges from 24 MPa to 32 MPa in areas farther from the excavations. In contrast, in areas adjacent to the openings, the stress magnitudes range from 32 MPa to 40 MPa, as shown in Figure 12, which represents the Vanesa sector.

According to empirical rockburst assessment methods (Zhou et al., 2018, He et al., 2023) based on the maximum tangential stress and the intact rock strength, like the Russenes (1974) or Hou et al. (1992), the rockburst potential varies from medium to strong intensity.

When seismicity can be correlated with the volume of rock extracted in each productive blast, controlling the extracted volume can effectively manage seismic risk. In such scenarios, the extraction of rock induces stress intensification and redistribution around the opening. The excess stress generated must be dissipated to achieve a stable equilibrium within the rock mass. This dissipation occurs through brittle plastic failure manifested in the mine as induced seismicity and induced damage. Once the excess stress is fully dissipated, seismicity ceases. To correctly associate blasting and

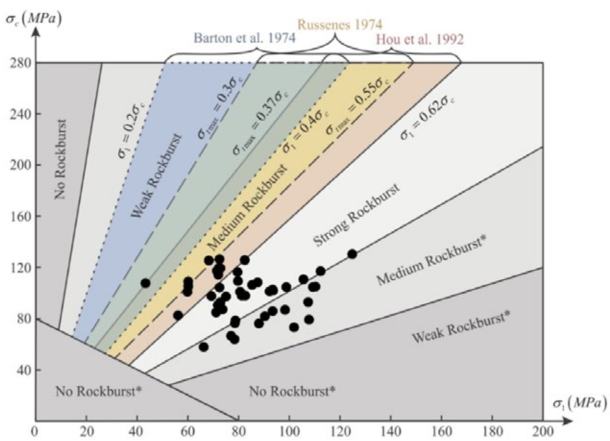

Figure 13—Empirical evaluation of rockburst potential based on the criteria proposed by Russenes (1974) and Hou et al. (1992) (Modified from Zhou et al., 2018)

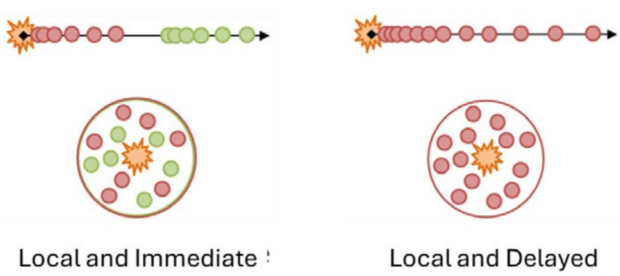

Figure 15—Graphical description of local-immediate and local-delayed seismic response, with a time scale in the upper part of the figure and a spatial diagram in the bottom part (modified from Woodward and Wesseloo, 2015)

seismicity it is necessary to correctly define the seismic response associated with each blast, for each seismogenic domain.

Method application

Seismic source mechanism and relationship with mined volume

Because of the diversity of seismic responses (and mechanisms) observable in the Raura mine, it is necessary to differentiate different sectors based on the seismic response characteristics observed and their relation to mine production.

The definition of the failure mechanism

When seismicity is directly related to blasting, it is possible to generate a relation between the metric tonnes extracted and the seismic deformation, represented here by the cumulative seismic moment, which also allows one to obtain a seismic rate as a function of production. In this case, one can obtain the seismic moment generated (Nm) per metric tonne of rock extracted (t).

To achieve this relation, it is fundamental to consider blasts and seismicity for a rock volume with characteristic seismic responses. This is because there are zones in the massif with a strong seismic response, while others do not generate seismicity, together with intermediate situations. It is necessary to identify these zones to achieve a positive relation between seismicity and production. This selection of analysis volumes is grounded in three fundamental aspects:

Spatial location

Spatial groupings of events tend to be associated with the same rupture mechanism, which physically occurs in a position within space. This spatial location may be local and immediate after blasting, but also can be delayed after blasting, as described by Woodward and Wesseloo 2015, where it is identified that these seismic responses are related to the stress distributions after blast and to the aftershocks after large induced seismic events, as shown in Figure 15.

Source mechanism from Gutenberg-Richter model

After isolating a rupture mechanism, the seismic events of the frequency-magnitude relationship must align according to the Gutenberg-Richter model. Deviations from this linearity arise because different rupture mechanisms are being considered in the database, making a temporospatial subdivision necessary (Figure 16).

Seismic moment/production ratio

When mine production information is available with location, tonnage, and extraction dates, we seek to define a volume with the greatest correspondence between tonnage extracted and seismicity generated. Figure 17 shows an example of three zones used for this study, segregating the blasts and seismicity of each volume. It should be mentioned that the best volume segregation for analysis is achieved after an iterative process, where initial volumes are selected but are then modified as a function of the previously described steps, seeking the best relation between mining and seismicity in compromise with the geological characteristics of the deposit and the seismic events' locations.

Within each of these zones, we calculate the cumulative tonnes and compare them with accumulated seismic moment, making it likely that a similar response will arise in both behaviours. If the

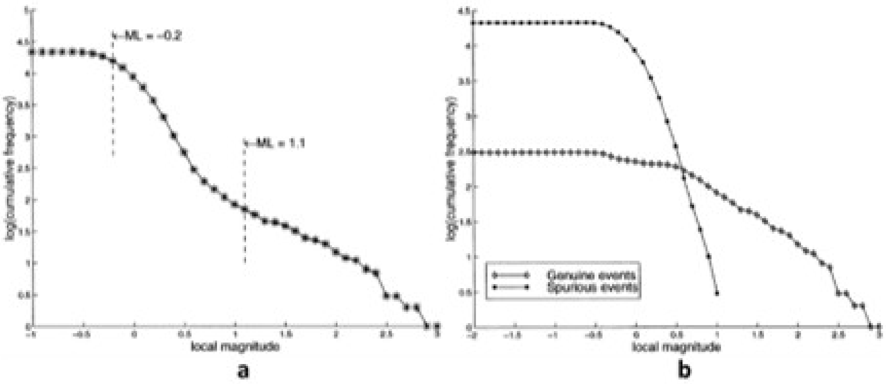

Figure 16—Example of mixed source mechanisms (a) and decomposition into two different frequency magnitude curves, one for each mechanism. Note that mixed mechanisms do not show a linear behaviour but isolated mechanism do behave linearly (After Woodward and Tierney, 2017)

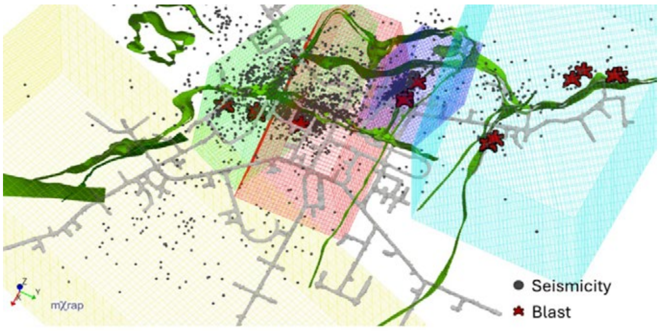

Figure 17—Example of several control volumes considering blasts and induced seismicity

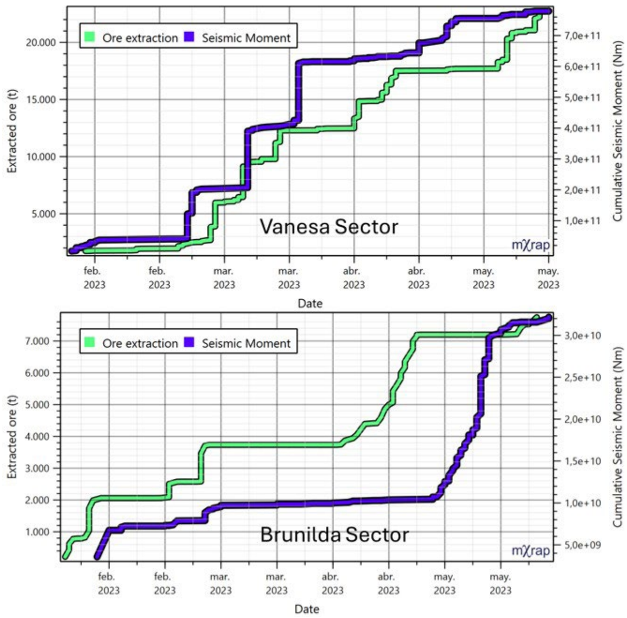

Figure 18—Example of temporal evolution within the Vanessa and Brunilda sectors: green line is production for each sector; blue line indicates cumulative seismic moment

response is not equivalent, the analysis volume must be redefined. To illustrate, we show the Vanessa and Brunilda sectors (Figure 18), indicating that cumulative seismic moment (blue line) increasing in close relation with blasting (green line).

Based upon this type of analysis, it is possible to obtain a linear relation between production in tonnes and seismic moment within

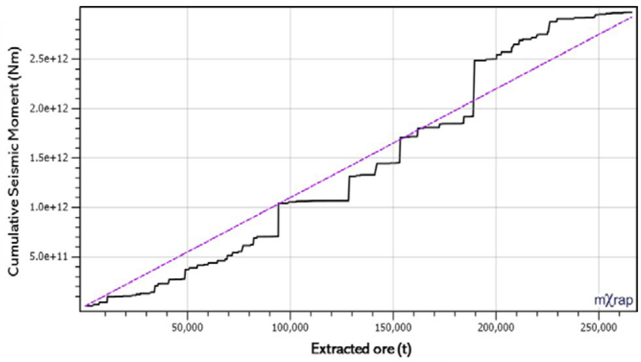

Figure 19—Relationship between seismic moment and extracted ore for all of Raura mine. This procedure has been replicated for all different seismogenic domains

the zone, which can be obtained for each mine sector. To illustrate, Figure 19 shows the relation obtained for the entire mine (all production vs all seismicity), obtaining the constants which define the line, so that:

$$MoEst = a + mP_{Min} \quad [4]$$

Where:

MoEst: Seismic moment (in Nm) estimate for a given production plan.

Pmin: mine production in tonnes.

a: Empirical constant for the line equation.

m: Empirically obtained slope of the linear trend.

When Equation 4 is defined for each control volume, one can obtain the production/seismicity relation for each sector, which can be shown as continuous lines, as indicated in Figure 20. This can be compared with historic information from mines in Canada (circles) and Australia (points) on the same graph, where one can conclude that only the Vanessa sector has a relatively high seismicity level.

The previously defined seismogenic domains (control volumes with distinctive characteristics) indicate that in the Raura mine, for the analysed timeframe, there are 4 sectors with a distinctive seismic behaviour (Hadas, Brunilda, Margot, and Vanesa). This characterisation of seismic behaviour is based on the inspection of the following seismic parameters:

For the current mine conditions, results show sectors with considerably low b-values, associated with high displacement in discontinuities (Wesseloo, 2014), particularly in reverse faults and

Table 1

Seismic characteristics measured based on recorded seismicity and current mine production

Seismogenic domain	b value (Gutenberg Richter)	Probability of seismic events greater than 2	Probability of events greater than 1 outside blasting hours	Seismic moment (Nm) per metric tonne extracted
Vanesa	0.85	46%	12%	36.000
Brunilda	1.0	5%	5%	3.100
Total mine	0.81	12%	15%	11.000

Table 2

Total expected momentum magnitude for each proposed seismogenic domain

	Monthly production (t)					Seismogenic domain
	100	1000	3000	5000	15000	
Total expected moment magnitude	0.3	0.9	1.3	1.4	1.7	Vanesa
	-0.2	0.5	0.8	1	1.3	Margot
	-0.4	0.2	0.5	0.7	1	Hadas
	-0.1	0.6	0.9	1.1	1.4	All mine

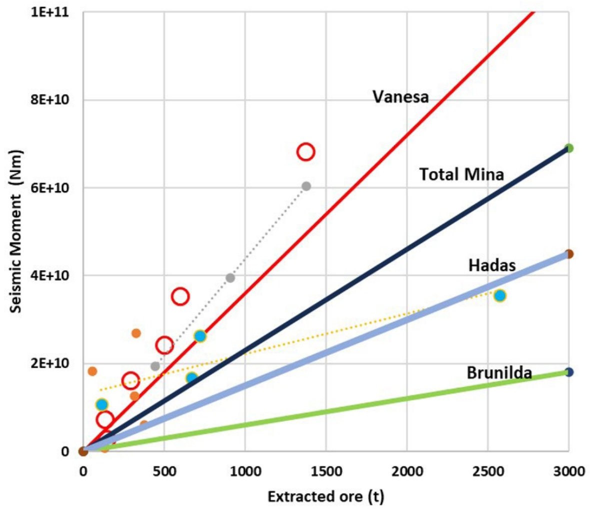

Figure 20—Relation between seismicity and mining for various productive sectors in the Raura mine

strike-slip faults (Vallejos, Estay, 2018), which can be associated with blocks displacement towards the interior of the generated cavities, as described in other cases worldwide by Linzer et al. (2020). Seismic events' time distribution also indicates that they mostly occur very close to blasting times, which is typical for a stress redistribution process after excavation. Given these elements, and considering the principal seismic rupture mechanisms accepted within the mining-induced seismicity area (Gibowcz, Kijko, 1994; Hoffman, Sheepers, 2011; Sjöberg et al., 2012; Potvin et al., 2010; Jarufe, 2020), one can conclude that seismicity in Raura is caused by the excavation-induced stresses, which mobilise structural planes near the open stopes, taking advantage of the loss of confinement by the excavations and the free face, which is generated in order to generate seismic rupture in the planes of pre-existing structural systems and mobilising blocks towards the volume generated by the open stopes, therefore timing backfill and limits to excavation rates should apply to assess seismic risk at Raura.

Calculate total seismicity for different mine planning scenarios

From the leftmost column in Table 1, one can calculate the amount of total seismic deformation (expressed as seismic moment) for a specific blasted in situ rock volume. In this exercise, several mine exploitation scenarios will be evaluated considering different monthly mining rates (Table 2).

The total co-seismic deformation is calculated for each planning scenario; however, since the total seismic moment for each scenario can be an unfamiliar value for most of rock mechanics and planning practitioners, the total seismic moment will be transformed to an equivalent moment magnitude following the relation proposed by Hanks and Kanamori (1979) where:

$$M_{We} = \frac{2}{3} * \log(Mo) - 6.01 \quad [5]$$

Where Mwe is the equivalent moment magnitude and Mo the total seismic moment released during the period considered in the mine plan scenario. Following this idea, Mwe is a moment magnitude equivalent to all the ruptures that occur during one mining period (one month in this case). The equivalent moment magnitude for all the planning scenarios on the different seismogenic domains can be seen in Table 2.

The equivalent magnitude from Table 2 represents the total co-seismic deformation occurring during a one-month period, as a single equivalent seismic event. This situation may be practical to get an order of magnitude of the seismicity occurring in each mining scenario, but real seismicity occurs as a series of several hundreds of exponentially distributed seismic events with an inverse cumulative distribution described by the GR relationship. This GR relationship for each mining scenario is the base for the seismic hazard calculation described in Equation 3, leading to the calculation of the probability that the maximum event will exceed a specified magnitude.

Develop probabilistic hazard model associated with each planned scenario

The probabilistic distribution of the largest expected events, described in Equation 3 is based on the GR parameters obtained from the frequency magnitude relationship. To evaluate the seismic hazard for different planning scenarios, GR parameters need to be estimated based on the available data. In this case, b-value (related to source mechanism) is obtained from current seismic data and the a-value (related to the number of events) is obtained utilising the method described by Jarufe et al. (2022) where a simplex optimisation algorithm is utilised to calculate values that generate a distribution of seismic events that are equivalent to the Mwe for each planning scenario.

Following this method, the probability distribution of the largest event occurrence, for each planning scenario is calculated, as illustrated in Figure 21 where the GR distribution is plotted (black line) and the probability distribution of the largest expected magnitude is shown as a coloured line on the right axis.

The previous procedure produces the complete exceedance probability of the possible largest event, however, for most mines it is only necessary to evaluate the probability of exceeding only specific magnitudes. In this case study, we carry out the comparison with the existing energy dissipation capacity in current developments, allowing us to evaluate whether the proposed mining plan generates seismic events, which can be contained by the current support system, or if additional investment is needed for supports to avoid potential block collapses, which can impede mining operations and harm workers. The magnitude of interest corresponds to 0.5, which is related to a medium risk level according to the mine experience; 2.0, corresponding to a high risk according to the mine experience; while 2.5 is an extreme magnitude. While the probabilities can be calculated for each seismogenic domain, only the global mine seismic hazard will be presented in this illustrated example, considering the annual probability of exceeding a specific magnitude for a specific monthly production rate, as shown in Figure 22.

With the probabilistic data on maximum magnitude for each plan in each sector, we can carry out the comparison with the existing energy dissipation capacity in current developments, allowing us to evaluate whether the proposed mining plan generates earthquakes, which can be contained by the current system or if additional investment is needed in supports to avoid potential block collapses, which can impede mining operations and harm workers.

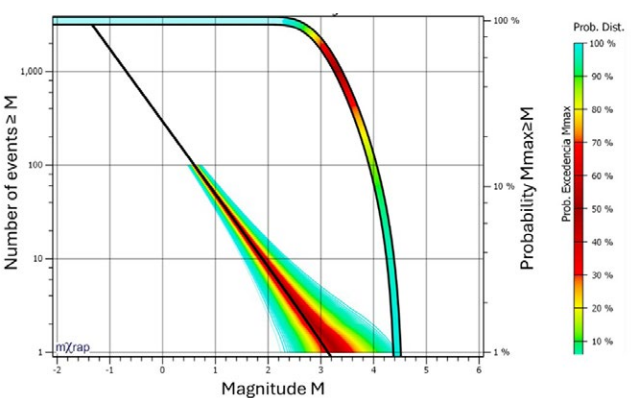

Figure 21—Probabilistic distribution of extreme magnitudes for one of the planning scenarios

Analysis and further work

This paper presents a method to evaluate the seismic hazard of different mining rates. While the evaluation of seismic potential has already been proposed by several authors, the practical relationship between a probability of exceeding a specific seismic magnitude associated with a mining plan has never been addressed directly. It is important to note that this paper addresses the seismic event occurrence, which does not necessarily become a rockburst. Therefore the probability of experiencing a rockburst will be lower than the results from this method. The method presented in this paper provides valuable insights regarding at which maximum rates each sector should be mined, and also provides guidelines to avoid areas without backfill. Furthermore, the use of mitigation techniques to reduce the rockburst consequences, as yielding support, post blast exclusion zones or rockmass preconditioning will reduce the rockburst probability even more.

Conclusions

This study has demonstrated a methodology for leveraging historical production and seismicity data from a mining operation to establish guidelines for mining rates and extraction strategies. The goal is to ensure operations are conducted within an acceptable risk level for the company. By applying extreme value theory and the classic Gutenberg-Richter relationship, the seismic hazard was probabilistically assessed. This approach was exemplified through a real-world application at the Raura mine in Peru.

We trust this methodology will be applied to other mining methods to further validate its utility, enabling the development of mining practices in a safe environment for workers while enhancing the economic value of mining operations.

Acknowledgments

The authors of this work would like to thank the Peru and Chile branches of REDCO and the Raura Mining Company for allowing this study to be published. Thanks is also due to the University of Santiago for funding.

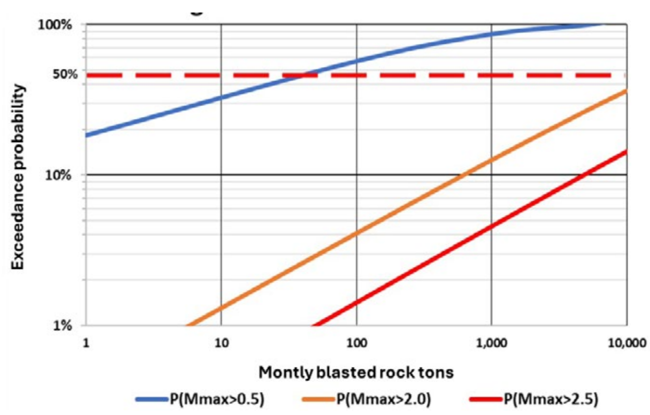

Figure 22—Exceedance probability for magnitudes 0.5, 2, and 2.5 for different monthly mining rates. This chart represents the average behaviour of the whole mine; however, specific charts for each seismogenic domain are recommended

References

An, H., Mu, X. 2024. *Contributions to Rock Fracture Induced by High Ground Stress in Deep Mining*: A Review. Rock Mech Rock Eng (2024). https://doi.org/10.1007/s00603-024-04113-z

Blake, W., Hedley, D.G. 2003. Rockbursts: case studies from North American hard-rock mines. Littleton: SME.

Cook, N. G. W. (1976). Seismicity associated with mining. *Engineering Geology*, vol. 10, no. 2-4, pp. 99-122. https://doi.org/10.1016/0013-7952(76)90015-6

Das Jennifer, P., Porchelvan, P., Naik, S.R. 2021. Numerical modelling of mining induced seismicity in deep closed mines: A case study. In International Conference on Geotechnical Challenges in Mining, Tunneling and Underground Infrastructures pp. 437-455. Singapore: Springer Nature Singapore.

Gibowicz, S. 1963. Magnitude and energy of subterrane shocks in Upper Silesia. *Studia Geophysica et Geodaetica*, vol.7, pp.1-37. https://doi.org/10.1007/BF02607768

Gibowicz, S.J., Kijko, A. 1994. *An Introduction to Mining Seismology*. Warsaw: Academic Press.

Glazer, S. N. (2016). *Mine Seismology: Data Analysis and Interpretation. Palabora Mine Caving Process as Revealed by Induced Seismicity*. New York: Springer International.

Glowacka, E. 1993. Probabilistic Seismic Hazard Evaluation in Underground Mines. *Natural Hazards*, vol. 7, no. 2, pp. 121-132.

Głowacka, E., Kijko, A. 1989. Continuous evaluation of seismic hazard induced by the deposit extraction in selected coal mines in Poland. In S. J. Gibowicz (Ed.), *Seismicity in Mines* pp. 523-533. Basel: Birkhäuser Basel.

Gutenberg, B., Richter, C.F. 1956. *Magnitude and Energy of Earthquakes. Nature*, pp. 176, 795. https://doi.org/10.1038/176795a0

Hanks, T.C., Kanamori, H. 1979. A moment magnitude scale. *Journal of Geophysical Research: Solid Earth*, vol. 84, (B5), pp. 2348-2350. https://doi.org/10.1029/JB084iB05p02348

Hasegawa, H.S., Wetmiller, R.J., Gendzwill, D.J. 1989. Induced seismicity in mines in Canada—an overview. *Pure and Applied Geophysics*, vol. 129, pp. 423-453. https://doi.org/10.1007/BF00874518

He, M., Cheng, T., Qiao, Y., Li, H. 2023. A review of rockburst: Experiments, theories, and simulations. *Journal of Rock Mechanics and Geotechnical Engineering*, vol. 15, no. 5, pp. 1312-1353.

Hou, F., Liu, X., Wang, M. 1992."Discussion on rockburst origin and degree." Proceedings of the 3rd Academic Conference on National Rock Dynamics. Technical University of Surveying and Mapping Press, Wuhan. 1992.

Hudyma, M. 2010. Applied Mine Seismology Concepts and Techniques. Technical notes for ENGR 5356. Mine Seismic Monitorting Systems, Laurentian Universtity

Hudyma, M., Potvin, Y.H. 2010. An Engineering Approach to Seismic Risk Management in Hardrock Mines. *Rock Mechanics and Rock Engineering*, vol. 43, pp. 891–906 (2010). https://doi.org/10.1007/s00603-009-0070-0

Jarufe, J. 2020. Fault slip seismicity in underground mining operations: asperity and barrier shear modelling. PhD Thesis, The University of Western Australia.

Jarufe, J., Perez, S., Hurtado, J.P., Cifuentes, C. 2022. Seismic hazard calculation using the equivalent magnitude obtained from numerical modelling. *International Journal of Rock Mechanics and Mining Sciences*, vol. 153, pp. 105081. https://doi.org/10.1016/j.ijrmms.2022.105081

Khalil, H., Chen, T., Xu, Y.H., Mitri, H. 2022. Effect of mining and geology on mining-induced seismicity–A case study. *Journal of Sustainable Mining*, vol. 21, no. 3, pp. 5. https://doi.org/10.46873/2300-3960.1361

Linzer, L.M., Hildyard, M.W., Spottiswoode, S.M., Wesseloo, J. 2020. Do stopes contribute to the seismic source? The Southern African Institute of Mining and Metallurgy, vol. 120, no. 1, pp. 81–90. http://doi.org/10.17159/2411-9717/954/2020

Malovichko, D. 2020. Description of seismic sources in underground mines: Theory. *Bulletin of the Seismological Society of America*, vol. 110, no. 5, pp. 2124-2137. https://doi.org/10.1785/0120200093

Martinsson, J., Törnman, W. 2020. Modelling the dynamic relationship between mining induced seismic activity and production rates, depth and size: a mine-wide hierarchical model. *Pure and Applied Geophysics*, vol. 177, no. 6, pp. 2619-2639. https://doi.org/10.1007/s00024-019-02378-y

McGarr, A. 1976. Seismic moments and volume changes. *Journal of Geophysical Research*, vol. 81, no. 8, pp. 1487-1494. https://doi.org/10.1029/JB081i008p01487

Mendecki, A.J. 2012. Size distribution of seismic events in mines. In Proceedings of the Australian Earthquake Engineering Society 2012 Conference, Queensland pp. 1-20.

Mendecki, A.J. 2013. *Characteristics of seismic hazard in mines*. 8th International Symposium on Rockbursts and Seismicity in Mines pp. 275-292, Russia.

Mendecki, A.J., Lötter, E.C. 2011. *Modelling seismic hazard for mines*. Australian Earthquake Engineering Society Conference pp. 18-20, Barossa Valley, South Australia.

Mendecki, A.J. 2016. Mine Seismology Reference Book, Seismic Hazard. Published by Institute of Mine Seismology.

Mendecki, A.J. 2023. Seismic ground motion alerts for mines. Journal of Seismology, vol. 27, no. 4, pp. 599-608.

Orlecka-Sikora, B., Lasocki, S., Lizurek, G., Rudziński, Ł. 2012. Response of seismic activity in mines to the stress changes due to mining induced strong seismic events. International Journal of Rock Mechanics and Mining Sciences, vol. 53, pp. 151-158. https://doi.org/10.1016/j.ijrmms.2012.05.010

Ortlepp, W.D. 1997. Rock Fracture and Rockbursts-An Illustrative Study. Monograph Series/South African Institute of Mining and Metallurgy.

Potvin, Y., Jarufe, J., Wesseloo, J. 2010. Interpretation of seismic data and numerical modelling of fault reactivation at El Teniente, Reservas Norte sector. *Mining Technology,* vol. 119, no. 13, pp. 175–181. https://doi.org/10.1179/174328610X12820409992453

REDCO. 2021. Reporte Tecnico, Dimensionamiento de Unidades Básicas de Explotación. Internal Report.

Russenes, B.F. 1974. Analysis of Rock Spalling for Tunnels in Steep Valley Sides (in Norwegian). Master's Thesis, Norwegian Institute of Technology, Department of Geology, Norway, 247.

Sjöberg, J., Perman, F., Quinteiro, C., Malmgren, L., Dahnér-Lindkvist, C., Boskovic, M. 2012. Numerical analysis of alternative mining sequences to minimise potential for fault slip rockbursting. Mining Technology, vol. 121, no. 4, pp. 226-235.

Vallejos, J.A., Estay, R.A. 2018. Seismic parameters of mining-induced aftershock sequences for re-entry protocol development. Pure and applied geophysics, vol. 175, pp. 793-811.

Vallejos, J.A., McKinnon, S.D. 2011. Correlations between mining and seismicity for re-entry protocol development. International Journal of Rock Mechanics and Mining Sciences, vol. 48, (no. 4, pp. 616-625.

Van Aswegen, G., Butler, A. 1993. Applications of quantitative seismology in South African gold mines. Rockbursts and seismicity in mines, vol. 93, pp. 261-266.

Vatcher, J., Boskovic, M., Sjöberg, J. 2019. Production-associated risk factors of seismicity in the Kiirunavaara mine. MGR 2019: Proceedings of the First International Conference on Mining Geomechanical Risk pp. 261-272, Perth.

Viljoen, N., Buss, B., Lafleur, C. 2021. Stope Dimension Evaluation Tool (SDET). CIM Conference, Canada.

Wagner, H. 2019. Deep mining: a rock engineering challenge. *Rock Mechanics and Rock Engineering*, vol. 52, pp. 1417-1446.

Wang, G., Kaiser, P.K., Vasak, P. 2009. Modeling of mining-induced seismicity migration. *ROCKENG09: Proceedings of the 3rd CANUS Rock Mechanics Symposium*, Toronto.

Wesseloo, J. 2014. Evaluation of the spatial variation of b-value. *The Journal of The Southern African Institute of Mining and Metallurgy*, vol. 114, no. 10, pp. 823–828.

Wesseloo, J. 2020. Addressing misconceptions regarding seismic hazard assessment in mines: b-value, Mmax, and space-time normalization. Journal of the Southern African Institute of Mining and Metallurgy, vol. 120, no.1, 67-80.

Woodward, K.R., Tierney, S.R. 2017. Seismic hazard estimation using databases with bimodal frequency–magnitude behaviour. In UMT 2017: Proceedings of the First International Conference on Underground Mining Technology (pp. 219-232). Australian Centre for Geomechanics.

Woodward, K., Wesseloo, J. 2015. Observed spatial and temporal behaviour of seismic rock mass response to blasting. *Journal of the Southern African Institute of Mining and Metallurgy*, vol. 115, no. 11, pp. 1044-1056.

Zhou, J., Li, X., Mitri, H.S. 2018. Evaluation method of rockburst: state-of-the-art literature review. Tunnelling and Underground Space Technology, vol. 81, pp. 632-659. https://doi.org/10.1016/j.tust.2018.08.029 ◆